
Building effective deep neural network architectures one feature at a time

Martin Mundt

Frankfurt Institute for Advanced Studies
Ruth-Moufang-Str. 1
60438 Frankfurt, Germany
mundt@fias.uni-frankfurt.de

Tobias Weis

Goethe-University Frankfurt
Theodor-W.-Adorno-Platz 1
60323 Frankfurt, Germany
weis@ccc.cs.uni-frankfurt.de

Kishore Konda*

INSOFE
Janardana Hills, Gachibowli
500032 Hyderabad, India
kishore.konda@insofe.edu.in

Visvanathan Ramesh

Frankfurt Institute for Advanced Studies
Ruth-Moufang-Str. 1
60438 Frankfurt, Germany
ramesh@fias.uni-frankfurt.de

Abstract

Successful training of convolutional neural networks is often associated with the training of sufficiently deep architectures composed of high amounts of features while relying on a variety of regularization and pruning techniques to converge to less redundant states. We introduce an easy to compute metric, based on feature time evolution, to evaluate feature importance during training and demonstrate its potency in determining a networks effective capacity. In consequence we propose a novel algorithm to evolve fixed-depth architectures starting from just a single feature per layer to attain effective representational capacities needed for a specific task by greedily adding feature by feature. We revisit popular CNN architectures and demonstrate how evolved architectures not only converge to similar topologies that benefit from less parameters or improved accuracy, but furthermore exhibit systematic correspondence in representational complexity with the specified task. In contrast to conventional design patterns that typically have a monotonic increase in the amount of features with increased depth, we observe that CNNs perform better when there is a peak in learnable parameters in intermediate, with falloffs to earlier and later layers.

1 Introduction

Estimating and consequently setting effective representational capacity in deep neural networks for any given task has been a long standing problem where fundamental understanding still seems to be insufficient to rapidly decide on suitable network sizes, topologies or even comprehension of why they work so well in practice. While widely adopted convolutional neural networks (CNNs) such as proposed by [1, 2, 3] demonstrate high accuracies on a variety of problems, the memory footprint and computational complexity vary. An increasing amount of recent work is already providing valuable insights and proposing new methodology to address these points. For instance, the authors of [4] propose a reinforcement learning based meta-learning approach to have an agent select potential CNN layers in a greedy, yet iterative fashion, other suggested architecture selection algorithms are more biologically inspired and draw their inspiration from concepts such as evolutionary synthesis [5, 6]. Although the former methods are capable of evolving architectures that rival those crafted by human design it is at this point in time only achievable at the cost of navigating large search spaces

*Work was conducted during time spent at Goethe-University Frankfurt.

and hence excessive computation and time. As a trade-off in present deep neural network design processes it thus seems plausible to consider layer types or depth of a network to be selected by an experienced engineer based on prior knowledge stemming from similar tasks and former research. A variety of techniques thus focus on improving already well established architectures. Procedures ranging from distillation of one network’s knowledge into another [7], compressing and encoding learned representations [8], pruning alongside potential retraining of networks [9, 10, 11, 12] and the employment of different regularization terms during training [13, 14, 15, 16], are just a fraction of recent efforts in pursuit of reducing representational complexity in order to achieve reduced storage and computational cost while essentially retaining accuracy. The underlying mechanisms rely on a multitude of criteria such as activation magnitudes [11] and small weight values [9] used as pruning metrics for either single neurons or complete feature maps, in addition to further combination with regularization and penalty terms.

Common to these works is the necessity of training large networks with huge parameter quantities for maximum representational capacity to full convergence. There thus is a need for an early identification of insufficient effective capacity and a conclusive increase in parameters. In this work we propose an intuitive, yet effective metric to evaluate feature importance in a neural network. In principle this measure is based on feature time evolution, that is the normalized cross-correlation of each feature with its reference initialization state, as a surrogate for active learning dynamics. We show how decisions on the necessary number of features can be based on this metric at any given point in time of training a fixed-depth architecture. After briefly evaluating the metric in context of pruning, we introduce a bottom-up approach in which we systematically evolve fixed-depth networks starting with a single filter per layer. We then proceed to revisit some of the most popular CNN architectures [1, 2, 3, 17] and show how automatically constructed networks of proposed types scale in terms of complexity for different datasets. In terms of accuracy developed architectures either maintain their reference accuracy at reduced amount of parameters or extend the network’s capacity to achieve better results. As the most interesting insight we provide an analysis of how evolved network topologies differ from their reference counterparts. Whereas conventional convolutional neural network architectures usually increase the amount of features monotonically with increased depth, we observe that automatically formed topologies exhibit maximal feature count at intermediate layers and then proceed to decrease in complexity.

2 Using weight-tensor cross-correlation to measure effective capacity

Deep neural networks only perform well if their capacity is chosen to approximately correspond to required complexity of a task given supplied data. While the choice and size of model indicate the *representational capacity* and thus determine which functions can be learned to improve training accuracy, training of neural networks is further complicated by the complex interplay of choice of optimization algorithm and model regularization that together define the *effective capacity*. This makes training of deep neural networks particularly challenging. One practical way of addressing this challenge is to boost model sizes at the cost of increased memory and computation times and then applying strong regularization to avoid over-fitting and minimize generalization error. However, this approach seems unnecessarily cumbersome and relies on the assumption that optimization difficulties are not encountered.

We draw inspiration from this challenge and propose a metric to gauge the effective capacity in the training of (deep) neural networks with stochastic gradient descent (SGD) algorithms. In SGD the objective function $J(\Theta)$ is commonly equipped with a penalty on the parameters $R(\Theta)$, yielding a regularized objective function:

$$\hat{J}(\Theta) = J(\Theta) + \alpha R(\Theta) . \tag{1}$$

Here, α weights the contribution of the penalty. The regularization term $R(\Theta)$ is typically chosen as an L_2 -norm, coined weight-decay, to decrease model capacity or a L_1 -norm to enforce sparsity. Methods like dropout [18] and batch normalization [19] can act as further regularizers.

As a surrogate measure for the effective capacity at a given state of learning, we propose to monitor the time evolution of the normalized cross-correlation for all weights with respect to their state at initialization. For a convolutional network composed of layers $l = 1, 2, \dots, L - 1$ and complementary weight-tensors $\mathbf{W}_{f^l j^l k^l f^{l+1}}^l$ with spatial dimensions $j^l \times k^l$ defining a mapping from an input feature-space $f^l = 1, 2, \dots, F^l$ onto the output feature space $f^{l+1} = 1, 2, \dots, F^{l+1}$ that serves as input to the

next layer, we define the following metric:

$$\mathbf{c}_{f^{l+1},t}^l = \frac{\sum_{f^l,j^l,k^l} \left[\left(\mathbf{W}_{f^l j^l k^l f^{l+1},t_0}^l - \bar{\mathbf{W}}_{f^{l+1},t_0}^l \right) \circ \left(\mathbf{W}_{f^l j^l k^l f^{l+1},t}^l - \bar{\mathbf{W}}_{f^{l+1},t}^l \right) \right]}{\left\| \mathbf{W}_{f^l j^l k^l, t_0}^l \right\|_{2, f^{l+1}} \cdot \left\| \mathbf{W}_{f^l j^l k^l, t}^l \right\|_{2, f^{l+1}}} \quad (2)$$

which is a measure of self-resemblance and will be referred to as the weights’ normalized cross-correlation. In this equation, $\mathbf{W}_{f^l j^l k^l f^{l+1},t}^l$ is the state of a layer’s weight-tensor at time t or the initial state after initialization t_0 , $\bar{\mathbf{W}}_{f^{l+1},t}^l$ is the mean taken over spatial and input feature dimensions, and \circ depicts the Hadamard product that we use in an extended fashion from matrices to tensors where each dimension is multiplied in an element-wise fashion analogously. Similarly the terms in the denominator are defined as the L_2 -norm of the weight-tensor taken over said dimensions and thus resulting in a scalar value. Above equation can be defined in the same way for linear layers and therefore multi-layer perceptrons by omitting spatial dimensions.

The rationale for the definition of the metric as portrayed in equation 2 is based on the following hypothesis: While a feature’s absolute magnitude or relative change between two subsequent points in time might not be adequate measures for direct importance, the relative amount of change a feature experiences with respect to its original state provides an indicator for how many times and how much a feature is changed when presented with data. Intuitively we suggest that features that experience high structural changes must play a more vital role than any feature that is initialized and does not deviate from its original states’ structure. There are only two potential reasons why a feature that has randomly been initialized does not change in structure: The first being that its form is already initialized so well that it does not need to be altered and can serve either as is or after some scalar rescaling or shift in order to contribute to the task. The second possibility is that too high representational capacity, the nature of the cost function, too large regularization or the type of optimization algorithm prohibit the feature from being learned, ultimately rendering it obsolete. As deep neural networks are commonly initialized from using a distribution over high-dimensional space the first possibility seems unlikely. The former factors have led us to the definition in equation 2, as normalized cross-correlation has an inherent invariance to effects such as translations or rescaling of weights stemming from regularization contributions. Therefore the contribution of the sum-term in equation 1 does not change the value of the metric if the gradient term vanishes.

2.1 Measuring feature importance

We first evaluate the use of equation 2 through the lens of pruning to demonstrate that our measure strongly correlates with feature importance. We have thus trained a five layer CNN-3C-2FC network,

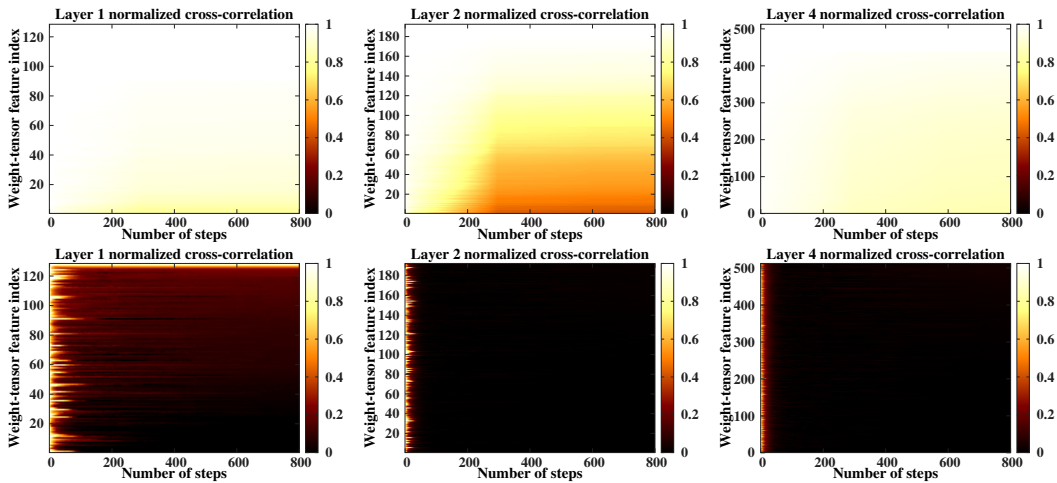


Figure 1: Time evolution of weight-tensor normalized cross-correlation for the CNN-3C-2FC architecture trained on MNIST (top row) and CIFAR-100 (bottom row) datasets using the initialization scheme proposed in [13]. The third layer, being similar in nature to the second, has been omitted and evolution has been discretized to 4 steps per epoch for ease of visualization.

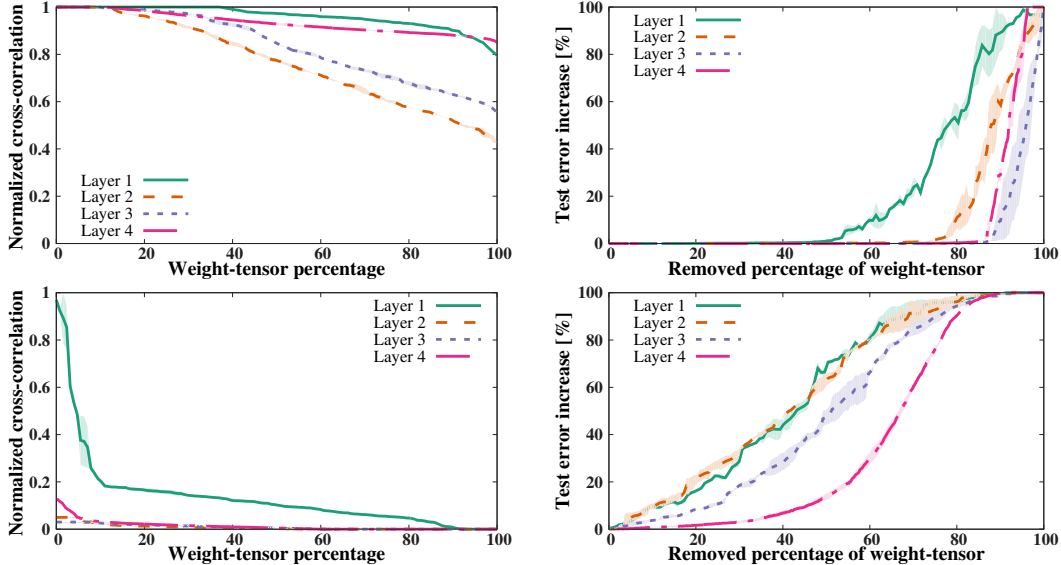


Figure 2: Greedy feature pruning for the CNN-3C-2FC architecture trained five times on MNIST (top row) and CIFAR-100 (bottom row) datasets. Left columns depict sorted mean normalized cross-correlation values at end of training for every layer. Right columns illustrate accuracy loss when removing features in descending order of normalized cross-correlation values. Shaded regions denote standard deviations. X-axes have been rescaled to a percentile view of features to enhance perception of differences between differently sized layers.

with three convolutional and two fully-connected layers, similar to [20] (but without the maxout operation) containing a set of $\{128, 198, 198, 512, 10\}$ features and following the initialization scheme proposed in [13], see supplementary material for precise training instructions, on both the MNIST [21] and the CIFAR-100 [22] datasets, expecting that such a network will be too large for the easier MNIST, and too small for the difficult CIFAR-100 task. In figure 1 the time evolution of $c_{f^{l+1}, t}^l$ is illustrated, where features are sorted in order of descending normalized cross-correlation value at the last training step. We observe that each layer exhibits a different amount of static filters for the MNIST training, whereas seemingly all features undergo rapid and harsh changes in CIFAR-100 training. In order to demonstrate that our measure is directly related to a feature’s importance and contribution to task performance we evaluate the contribution of the features by pruning the weight-tensor feature by feature in descending order of $c_{f^{l+1}, t_{end}}^l$ values and re-evaluating the remaining architecture on the testset. Architectures have been trained and pruned five times. The corresponding mean increase in error, relative to the maximally achieved accuracy, and respective standard deviation (shaded regions) are depicted in figure 2. Pruning any feature from the architecture trained on CIFAR-100 immediately results in loss of performance, whereas the architecture trained on MNIST can be pruned to a smaller set of parameters by simply greedily dropping the next feature with highest normalized cross-correlation value. The first major observation is that for the five runs of the network we see little deviations and the architectures always converge to very similar states, suggesting that our metric provides simple means to gauge effective capacity. Additional time evolutions as depicted in figure 1 can be found in the supplementary material section. We notice two additional distinct points: Any feature that has a cross-correlation value of 1, and thus has not been restructured during training, can be pruned in one-shot without loss in accuracy, validating our earlier formulated hypothesis that these features are in fact obsolete. The architecture could be pruned further, however at the cost of introducing different thresholds for each layer. A vast majority of parameters can be pruned in the last, fully-connected, layer. This is coherent with findings presented in [9], where the fully-connected layers show lowest sensitivity to pruning. In contrast to the former work, using our metric for pruning does not require any retraining of weights and is not based on pruning weights with low values or in fact low activation values. The interested reader is referred to the supplementary material for weight distribution and activity diagrams. We also show additional examples of the difference between the two initialization schemes and how the initialization of [23] systematically seems to require more features to achieve equal accuracies. We provide an algorithm to build a network starting with one

Algorithm 1 Greedy feature by feature architecture expansion algorithm

Require: Set hyper-parameters: Learning rate λ , batch size m , maximum epoch t_{end}, \dots

- 1: Initialize parameters $\Theta, t = 0, \epsilon = 10^{-6}, F^l = 1 \forall l = 1, 2, \dots, L - 1$
- 2: **while** $t \leq t_{end}$ **do**
- 3: Compute gradient and perform update step
- 4: Set $reset = false$
- 5: **for** $l = 1$ to $L - 1$ **do**
- 6: **for** $i = f^{l+1}$ to F^{l+1} **do**
- 7: Update $\mathbf{c}_{i,t}^l$ according to equation 2
- 8: **end for**
- 9: **if** $\max(\mathbf{c}_{i,t}^l) < 1 - \epsilon$ **then**
- 10: $F^{l+1} \leftarrow F^{l+1} + 1$
- 11: $reset = true$
- 12: **end if**
- 13: **end for**
- 14: $t \leftarrow t + 1$
- 15: **if** $reset == true$ **then**
- 16: Re-initialize parameters $\Theta, t = 0$
- 17: **end if**
- 18: **end while**

feature in every layer until a set of features that matches hypothesized effective capacity is reached and identify suitable network topologies.

2.2 Building networks bottom-up feature by feature

Contrary to pruning, we propose a new method to converge to architectures that encapsulate necessary task complexity without the necessity of training huge networks in the first place. Starting with one feature in each layer, we expand our architecture as long as the effective capacity as estimated through our surrogate metric is not met and all features experience change in all layers. In contrast to methods such as [4, 5, 6] we do not consider flexible depth and treat the amount of layers in a network as a prior based on the belief of hierarchical composition of the underlying factors. Our method, shown in algorithm 1, can be summarized as follows: For a given network arrangement in terms of function type and depth and a set of hyper-parameters, we initialize each layer with just one feature and proceed to follow a conventional optimization procedure for gradient descent algorithms. After each update step we then evaluate the metric independently per layer as described by equation 2 and increase feature dimensionality of respective layer by one if all currently present features are differing from their initial state by more than a constant ϵ in $\mathbf{c}_{f^{l+1},t}^l$. We note that this is a numerical stability parameter that we set to a small value such as 10^{-6} , but could in principle as well be used as a constraint if set to lower values. Even though our algorithm will not yield the smallest possible architectures as suggested in the previous section, we feel that this approach offers more value than setting individual layer sensitivity hyper-parameters. We have decided to include the re-initialization in lines 15 – 17 to avoid the pitfalls of falling into local minima. Despite this sounding like a major detriment to our method, we show that networks nevertheless rapidly converge to a stable architectural solution that comes at less than per chance expected computational overhead and at the benefit of avoiding training of too large architectures. Because our algorithm does not directly depend on gradient or higher-order term calculation, a major advantage is that computation of equation 2 can be done at less cost than a regular forward pass through the network and in principle only features that have not yet changed have to keep getting monitored as we are only interested in deviations from initial state.

3 Revisiting popular architectures

We revisit some of the most established architectures and compare achieved accuracies and number of learnable parameters with those obtained through evolved architectures that started from a single feature in each layer. As we would like to demonstrate how representational capacity in our

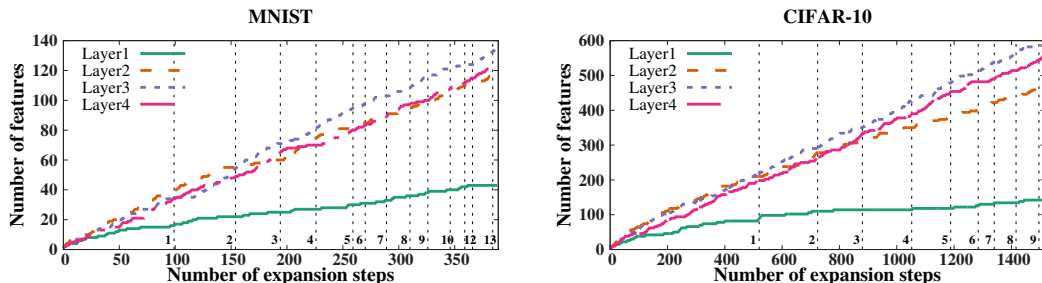


Figure 3: Examples for network expansion of the CNN-3C-2FC architecture on MNIST and CIFAR-10. Whereas the x-axis is labeled with absolute number of expansion steps, vertical dashed lines denote corresponding epochs. Expansion can be perceived to slow down with each subsequent epoch until eventually the architecture converges and trains without further expansion. For both cases a similar relative network topology evolves.

automatically constructed networks scales with increasing task difficulty, we perform experiments on the MNIST [21], CIFAR-10 and CIFAR-100 [22] datasets that intuitively represent little to high classification challenge. In order to show that our algorithm works for different sets of convolutional networks we have identified three different architectures:

- a three convolution layer network with larger filters followed by two fully-connected layers [20], that we refer to as CNN-3C-2FC, representing the family of rather shallow "deep" networks
- the VGG-A model [1], containing 8 convolutional and two hidden fully-connected layers with 512 each, as an example of stacking of layers towards deeper architectures
- the 28 convolutional layer deep wide residual network" (WRN-28) architecture proposed in [3]. Here we use, what the authors refer to as a "basic-form" featuring no bottlenecks and a width-factor of 4 as our reference for evaluation. When we evolve this network this implies an inherent coupling of layer blocks due to dimensional consistency constraints with outputs from identity mappings.

In order to analyze neural network topologies we furthermore investigate two extensions to previously described baseline architectures:

- For the shallow and VGG architecture we thus also include the all-convolutional version proposed by [17] where all pooling layers are replaced by convolutions with larger stride. Even though the value of more complex type of pooling functions in contrast to e.g. imposed max-pooling has already empirically been demonstrated [24], the amount of features of the replaced layers has been constrained to match in dimensionality with the preceding convolution layer. We would thus like to further extend and analyze the role of layers involving sub-sampling by decoupling the dimensionality of these larger stride convolutional layers.
- As a second extension we examine the role of fully-connected layers by entirely replacing them with a single convolution with spatial filter dimension corresponding to the entire spatial size of the output feature map of the previous layer. This last convolution is not followed by a non-linearity and thus represents a direct affine mapping onto the class space.

We will later see that these networks perform equally well or even better indicating that the classes are clustered well enough by a purely convolutional architecture so that a linear separation can easily be achieved. Although we are in principle able to achieve higher results with different sets of hyper-parameters and preprocessing methods, we limit ourselves to the training methodology presented in [2] and [3] to provide a comprehensive comparison. The exact training details can be found in supplementary material or in [3]. We train all architectures five times on each dataset, including reference architectures, as to the best of our knowledge there is no literature report with consolidated training methodology for all architectures. We apply analogous training procedure for our evolved architectures. Exemplary expansion processes that converge to architectures within few epochs are shown in figure 3. We emphasize that layers expand independently, yet converge to

Table 1: Mean error and mean number of parameters (in millions) for the different networks trained five times using the original reference and automatically expanded architectures respectively. For MNIST no data augmentation has been applied, and CIFAR-10 and CIFAR-100 datasets have been augmented using horizontal flips and up to four pixel random translations. For each of the three architectures, three variants, comprised of the standard architecture, an all-convolutional (all-conv) version as proposed by [17] and an all-convolutional version where fully-connected layers have been replaced with a single affine transformation (all-conv + no FC) have been evaluated.

type		CNN-3C-2FC		VGG-A-8C-3FC		WRN-28-4		
		original	expanded	original	expanded	original	expanded	
MNIST	standard	error [%]	0.360	0.340	0.329	0.318	0.307	0.264
		parameters	4.11M	1.1M	13.74M	3.35M	5.86M	4.83M
	all-conv	error [%]	0.341	0.347	0.341	0.333		
		parameters	5.11M	1.75M	15.12M	2.65M		
	all-conv + no FC	error [%]	0.355	0.322	0.345	0.324		
		parameters	3.56M	2.91M	11.43M	3.79M		
CIFAR-10 +	standard	error [%]	13.08	10.71	8.42	8.10	7.58	3.98
		parameters	4.11M	15.98M	13.74M	7.49M	5.86M	25.30M
	all-conv	error [%]	10.38	8.02	8.22	7.52		
		parameters	5.11M	16.67M	15.12M	14.73M		
	all-conv + no FC	error [%]	10.44	7.99	8.13	7.41		
		parameters	3.56M	18.99M	11.43M	11.68M		
CIFAR-100 +	standard	error [%]	33.33	30.53	26.55	25.35	21.73	18.34
		parameters	4.11M	20.13M	13.74M	10.81M	5.86M	27.75M
	all-conv	error [%]	30.00	27.38	26.48	23.00		
		parameters	5.11M	22.12M	15.12M	22.55M		
	all-conv + no FC	error [%]	29.68	27.53	26.01	22.64		
		parameters	3.56M	20.94M	11.43M	13.47M		

different points. We would like to further note that while late epoch re-initializations in algorithm 1 seem to occur in principle, we empirically observe that this rarely seems to be the case. Additional practical considerations can be found in the supplementary material section.

Table 1 shows all obtained results in terms of achieved mean error values and mean parameters over five runs of evaluated architectures. The general trend can easily be perceived: classification of MNIST seems to be a rather easy task in comparison to that of the CIFAR-10 and CIFAR-100 datasets which can be observed by the fact that all evolved architectures have equal or better performance at lower amount of parameters, whereas CIFAR-100 results are almost all improved using increased network capacity. We do also observe that the shallow architectures are able to gain much in terms of accuracy by massively increasing width and thus parameter count, although there seems to be a natural limit to what width can do in agreement with observations pointed out in other works such as [25, 26]. In comparison to results reported in [3] and [27] that both employ a WRN-28-10 and WRN-28-20 architecture featuring 36.55M and factor two times more parameters, we are able to obtain equal and even better results on the CIFAR-10 and CIFAR-100 datasets with much less parameters. In general we observe that this benefit is due to unconventional, yet always coinciding, network topology of our evolved architectures that suggest that there is more to CNNs than simply following the rule of thumb of increasing the number of features with increasing architectural depth. For reasons of clarity we do not report experiments containing extended methodology such as the oscillating learning rates proposed in [27] or better sets of hyper-parameters, even though accuracies rivaling state-of-the-art performances can be achieved in this way.

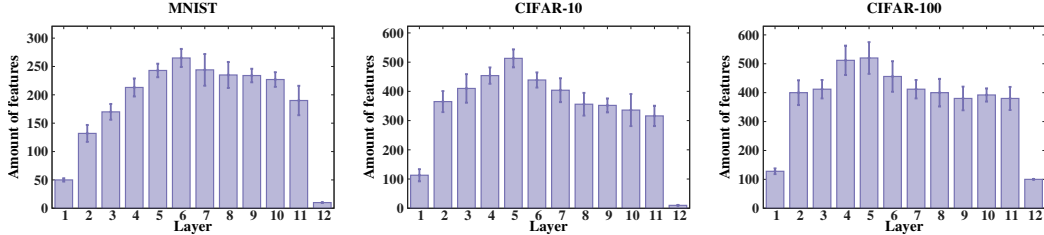


Figure 4: Mean and standard deviation of topologies as evolved from the expansion algorithm for a VGG-A all-convolutional architecture with fully-connected layers replaced by an affine transformation, run five times on MNIST, CIFAR-10 and CIFAR-100 datasets respectively.

4 Formation of deep neural network topologies

Almost all popular convolutional neural network architectures follow a design pattern of monotonically increasing feature amount with increasing network depth for all convolutional layers in the network [21, 20, 28, 29, 1, 17, 2, 3, 27, 26]. For the results presented in table 1 all evolved network topologies present alternatives to this pattern. We illustrate exemplary mean topologies for a VGG-A network trained on the three data sets by our evolution algorithm in five runs in figure 4. Apart from noticing the increase in representational capacity with dataset difficulty, we furthermore find topological convergence with small deviations from one training to another, as indicated by the errorbars. We observe the highest dimensionality in intermediate layers with decreasing dimensionality towards either end of the network differing from conventional CNN design patterns. This is a generally reoccurring behavior for all trained variants. Even if the evolved architectures sometimes do not deviate much from the original parameter count as can be seen for the CIFAR-10 VGG networks, accuracy is improved through this topological re-arrangement.

If we view the deep neural network as being able to represent any function that is limited rather by concepts of continuity and boundedness instead of a specific form of parameters, we can view the minimization of the cost function as learning a functional mapping instead of merely adopting a set of parameters [30]. We hypothesize that evolved network topologies containing highest feature amount in intermediate layers generally follow a process of first mapping into higher dimensional space to effectively separate the data into many clusters. The network can then more readily aggregate specific sets of features to form clusters distinguishing the class subsets. Empirically this behavior finds confirmation in all our evolved network topologies that are visualized in the supplementary part and in particular in our "all-conv + no FC" networks where we replaced the fully-connected layers by a single affine transformation. These networks have a linear mapping directly from the last convolutional layer onto the class space and can thus only work well if previously aggregated features are separable easily. However, we do not imply that fully-connected layers are useless altogether as they can play a potentially vital role in transfer learning and fine-tuning. Similar formation of topologies, restricted by the dimensionality constraint of the identity mappings, can be found in the trained residual networks. We furthermore notice how active paths taken in such networks are usually dominated by either the complete convolutional or skip connection alternative in ways very much alike the conclusions drawn in [31] and [32]. For future work it thus seems reasonable to analyze topological arrangement in networks such as proposed in "Densely Connected Convolutional Networks" [33], where skip connections are present but do not rely on matching dimensionality of subsequent layers.

5 Conclusion

In this work we have presented an easy to compute and intuitive metric to gauge the effective capacity of a neural network necessary for a given task. After briefly showing the metric as a monitor of training efficiency and demonstrating its capability in a pruning scenario or early prediction of under-fitting, we proposed an algorithm to build networks from bottom-up to converge to necessary capacity. The proposed algorithm leads to architectures that at times result in either significantly reduced amount of parameters or improved accuracies. This advantage seems to be gained through alternative network topologies with respect to commonly applied designs in current literature. Instead of increasing the amount of features monotonically with increasing depth of the network, we empirically observe that

effective neural network capacities demand to follow patterns to first map to high dimensional spaces and then start aggregation in the mapping process.

While this work has mainly focused on the metric and the interesting formation of neural network topologies, we have furthermore started to replace the currently present re-initialization step in our architecture evolution algorithm by keeping learned filters. In principle this approach looks promising but does need further systematic analysis of new feature initialization with respect to the already learned feature subset and accompanied investigation of orthogonality to avoid falling into local minima.

Acknowledgments

This project has received funding from the European Union’s Horizon 2020 research and innovation program under grant agreement No 687384. Kishora Konda received funding from Continental Automotive GmbH.

References

- [1] Karen Simonyan and Andrew Zisserman. Very Deep Convolutional Networks for Large-Scale Image Recognition. In *ICLR*, 2015.
- [2] Kaiming He, Xiangyu Zhang, Shaoqing Ren, and Jian Sun. Deep Residual Learning for Image Recognition. In *CVPR*, 2016.
- [3] Sergey Zagoruyko and Nikos Komodakis. Wide Residual Networks. In *BMVC*, 2016.
- [4] Bowen Baker, Otkrist Gupta, Nikhil Naik, and Ramesh Raskar. Designing Neural Network Architectures using Reinforcement Learning. *arXiv preprint arXiv:1611.02167*, 2016.
- [5] Mohammad J. Shafiee, Akshaya Mishra, and Alexander Wong. EvoNet: Evolutionary Synthesis of Deep Neural Networks. *arXiv preprint arXiv:1606.04393*, 2016.
- [6] Esteban Real, Sherry Moore, Andrew Selle, Saurabh Saxena, Yutaka Leon Suematsu, Quoc Le, and Alex Kurakin. Large-Scale Evolution of Image Classifiers. *arXiv preprint arXiv:1703.01041*, 2017.
- [7] Geoffrey E. Hinton, Oriol Vinyals, and Jeff Dean. Distilling the Knowledge in a Neural Network. In *NIPS Deep Learning Workshop*, 2014.
- [8] Song Han, Huizi Mao, and William J. Dally. Deep Compression - Compressing Deep Neural Networks with Pruning, Trained Quantization and Huffman Coding. In *ICLR*, 2016.
- [9] Song Han, Jeff Pool, John Tran, and William J. Dally. Learning both Weights and Connections for Efficient Neural Networks. In *NIPS*, pages 1135–1143, 2015.
- [10] Song Han, Huizi Mao, Enhao Gong, Shijian Tang, William J. Dally, Jeff Pool, John Tran, Bryan Catanzaro, Sharan Narang, Erich Elsen, Peter Vajda, and Manohar Paluri. DSD: Dense-Sparse-Dense Training For Deep Neural Networks. In *ICLR*, 2017.
- [11] Avanti Shrikumar, Peyton Greenside, Anna Shcherbina, and Anshul Kundaje. Not Just a Black Box: Interpretable Deep Learning by Propagating Activation Differences. In *ICML*, volume 1, 2016.
- [12] Li Hao, Asim Kadav, Hanan Samet, Igor Durdanovic, and Hans Peter Graf. Pruning Filters For Efficient Convnets. In *ICLR*, 2017.
- [13] Kaiming He, Xiangyu Zhang, Shaoqing Ren, and Jian Sun. Delving Deep into Rectifiers: Surpassing Human-Level Performance on ImageNet Classification. In *ICCV*, pages 2016–2034. IEEE Computer Society, 2015.
- [14] Guoliang Kang, Jun Li, and Dacheng Tao. Shakeout: A New Regularized Deep Neural Network Training Scheme. In *AAAI*, pages 1751–1757, 2016.
- [15] Pau Rodriguez, Jordi González, Guillem Cucurull, Josep M. Gonfaus, and Xavier Roca. Regularizing CNNs With Locally Constrained Decorrelations. In *ICLR*, 2017.
- [16] Jose M. Alvarez and Mathieu Salzmann. Learning the Number of Neurons in Deep Networks. In *NIPS*, 2016.
- [17] Jost T. Springenberg, Alexey Dosovitskiy, Thomas Brox, and Martin Riedmiller. Striving for Simplicity: The All Convolutional Net. In *ICLR*, 2015.
- [18] Nitish Srivastava, Geoffrey E. Hinton, Alex Krizhevsky, Ilya Sutskever, and Ruslan Salakhutdinov. Dropout : A Simple Way to Prevent Neural Networks from Overfitting. *JMLR*, 15:1929–1958, 2014.
- [19] Sergey Ioffe and Christian Szegedy. Batch Normalization: Accelerating Deep Network Training by Reducing Internal Covariate Shift. *arxiv preprint arXiv:1502.03167*, 2015.

- [20] Ian J. Goodfellow, David Warde-Farley, Mehdi Mirza, Aaron Courville, and Yoshua Bengio. Maxout Networks. In *ICML*, volume 28, pages 1319–1327, 2013.
- [21] Yann LeCun, Léon Bottou, Yoshua Bengio, and Patrick Haffner. Gradient-based learning applied to document recognition. *Proceedings of the IEEE*, 86(11):2278–2323, 1998.
- [22] Alex Krizhevsky. Learning Multiple Layers of Features from Tiny Images. Technical report, Toronto, 2009.
- [23] Xavier Glorot and Yoshua Bengio. Understanding the difficulty of training deep feedforward neural networks. *AISTATS*, 9:249–256, 2010.
- [24] Chen-Yu Lee, Patrick W. Gallagher, and Zhuowen Tu. Generalizing Pooling Functions in Convolutional Neural Networks: Mixed, Gated, and Tree. *Proceedings of the 19th International Conference on Artificial Intelligence and Statistics*, pages 464—472, 2015.
- [25] Lei J. Ba and Rich Caruana. Do Deep Nets Really Need to be Deep ? *arXiv preprint arXiv:1312.6184*, 2014.
- [26] Gregor Urban, Krzysztof J. Geras, Samira Ebrahimi Kahou, Ozlem Aslan, Shengjie Wang, Abdel-rahman Mohamed, Matthai Philipose, Matthew Richardson, and Rich Caruana. Do Deep Convolutional Nets Really Need To Be Deep And Convolutional? In *ICLR*, 2017.
- [27] Ilya Loshchilov and Frank Hutter. SGDR: Stochastic Gradient Descent With Warm Restarts. In *ICLR*, 2017.
- [28] Min Lin, Qiang Chen, and Shuicheng Yan. Network In Network. In *ICLR*, 2014.
- [29] Benjamin Graham. Fractional Max-Pooling. *arXiv preprint arXiv:1412.6071*, 2014.
- [30] Ian J. Goodfellow, Yoshua Bengio, and Aaron Courville. *Deep Learning*. MIT Press, 2016.
- [31] Rupesh Kumar Srivastava, Klaus Greff, and Jürgen Schmidhuber. Highway Networks. *arXiv preprint arXiv:1505.00387*, 2015.
- [32] Andreas Veit, Michael J. Wilber, and Serge Belongie. Residual networks behave like ensembles of relatively shallow networks. *NIPS*, pages 550–558, 2016.
- [33] Gao Huang, Zhuang Liu, and Kilian Q. Weinberger. Densely Connected Convolutional Networks. *arXiv preprint arXiv:1608.06993*, 2016.
- [34] Ronan Collobert, Koray Kavukcuoglu, and Clément Farabet. Torch7: A matlab-like environment for machine learning. *BigLearn, NIPS Workshop*, pages 1–6, 2011.

A Supplementary Material

A.1 Training details

Hyper-parameters: All training follows the procedure specified in [3]. In practice this means that we preprocess all data using global contrast normalization and actively refrain from other commonly employed forms of preprocessing such as ZCA-whitening or color transformations to spaces such as YUV. We furthermore follow the process of augmenting the CIFAR-10 and CIFAR-100 training by introducing horizontal flips and small translations of up to 4 pixels during training instead of following heavy data augmentation such as presented in [29]. No data augmentation has been applied to the MNIST dataset. All training has been conducted using a batch size of 128, a L_2 weight-decay of $5 \cdot 10^{-4}$, a batch normalization constant of $1 \cdot 10^{-3}$ and initial learning rates of 0.1 and 0.01 for the CIFAR and MNIST datasets respectively. In accordance with [3] a momentum of 0.9 and a learning rate schedule that reduces the learning rate by a factor of 5 whenever a multiple of 60 epochs has been trained, is applied. Weight initialization follows the initialization scheme proposed in [13]. In this fashion all networks have been trained five times for an overall amount of 200 epochs using a cross-entropy loss function. Similar in spirit to [28, 17], we implement fully-connected layers using convolutions with spatial dimensions 1×1 . Training has been conducted using a single NVIDIA Titan-X GPU and code has been written in Torch7 [34].

Practical considerations: We purposely refrain from reporting resulting compression values in this work as we believe the practice of training excessively large networks to report large pruning values is ill-posed as values are arbitrary in a sense that they depend only on the ability to regularize to an extreme. For our expansion algorithm we avoided suppression of late initialization behavior for all results reported in this work to exclude the possibility that rarely encountered worst-case behavior of restarting on an almost completely trained architecture provides any benefit, we advise that in practice later epochs could be prohibited from further network evolution. Along a similar line of thought a stability parameter ending the evolution early on could be introduced as a network that has been stable for multiple epochs does generally not appear to get trapped in local minima and very late allocation of features does not seem to improve generalization. It should also be noted that we add one feature at a time, but in principle speed-ups could be introduced by means of adding stacks of features.

A.2 Dependency on initialization

We show additional normalized cross-correlation time evolutions as depicted in figure 1 for both the initialization scheme suggested in [13] and [23] in figure 5. We observe that multiple runs of training with the same training configuration and dataset do result in time evolutions that look remarkably alike. We also notice that all architectures that we have trained with the initialization of [23] seem to require a larger amount of features to converge to the same performance for any given task and architecture.

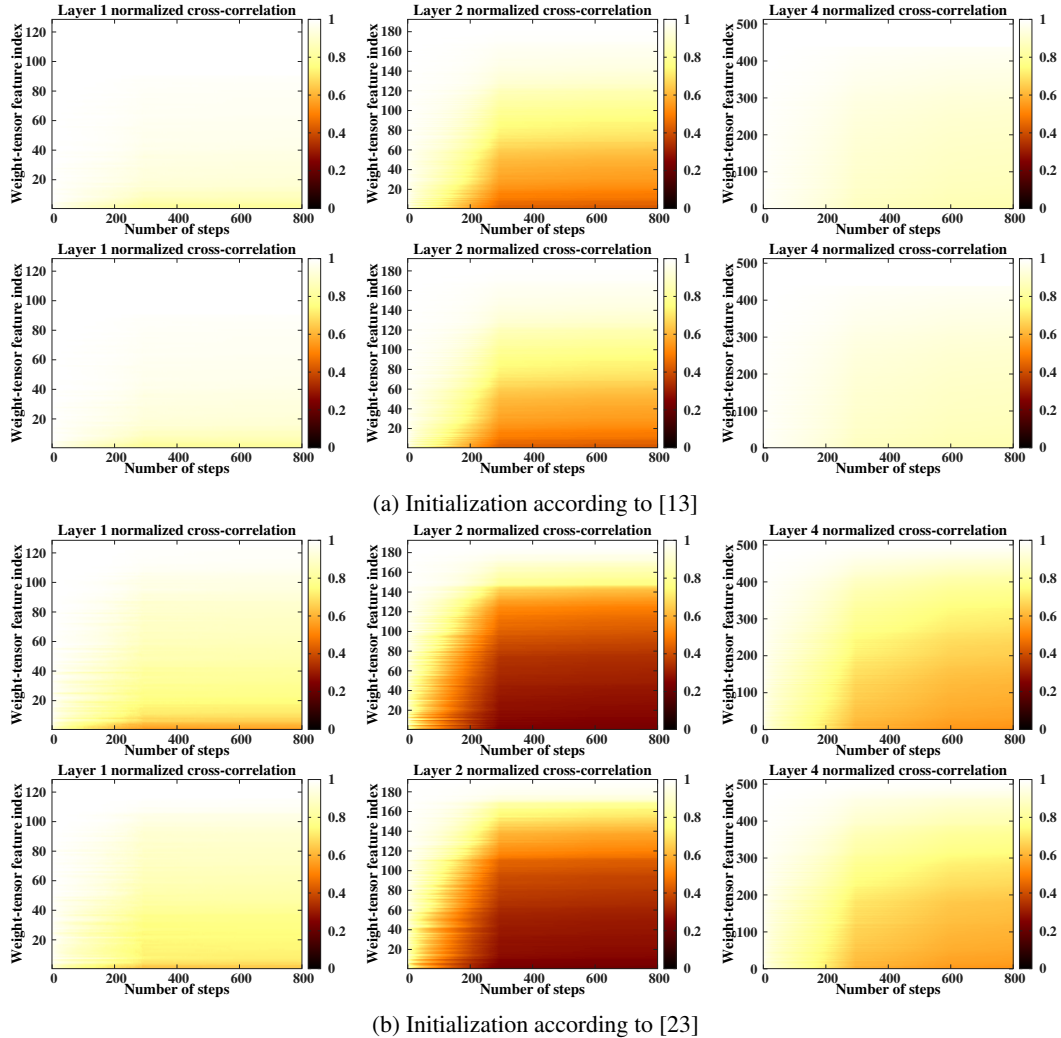


Figure 5: Time evolution of weight-tensor normalized cross-correlation for the CNN-3C-2FC architecture trained on the MNIST dataset. The top two rows use the initialization scheme proposed in [13], whereas the bottom two rows were initialized as suggested in [23]. The third layer, being similar in nature to the second, has been omitted and evolution has been discretized to 4 steps per epoch for ease of visualization.

A.3 Relation to neuron activity and weight values

We present that our metric defined in equation 2 does not rely on low activation values or small weight values to gauge a feature’s importance in contrast to other works such as [9] or [11].

Neuron activity: For the normalized cross-correlation time evolution shown in figure 1 we furthermore illustrate corresponding summed and normalized feature map activations for each epoch in figure 6. Here, features are presented in the same order as our sorted cross-correlation visualization. It is clearly visible that the pattern of activations does not follow that of the normalized cross-correlation evolution and values do not seem to correlate. Additionally, we see that relating low activation values with obsolescence of features might be misleading as we have shown in figure 2 that excluding any feature from this architecture trained on CIFAR-100 leads to reduced accuracy. Yet many low amplitude feature maps can be found in the bottom row of figure 6, suggesting that considering magnitude alone, at least on a level of entire feature maps, is not sufficient.

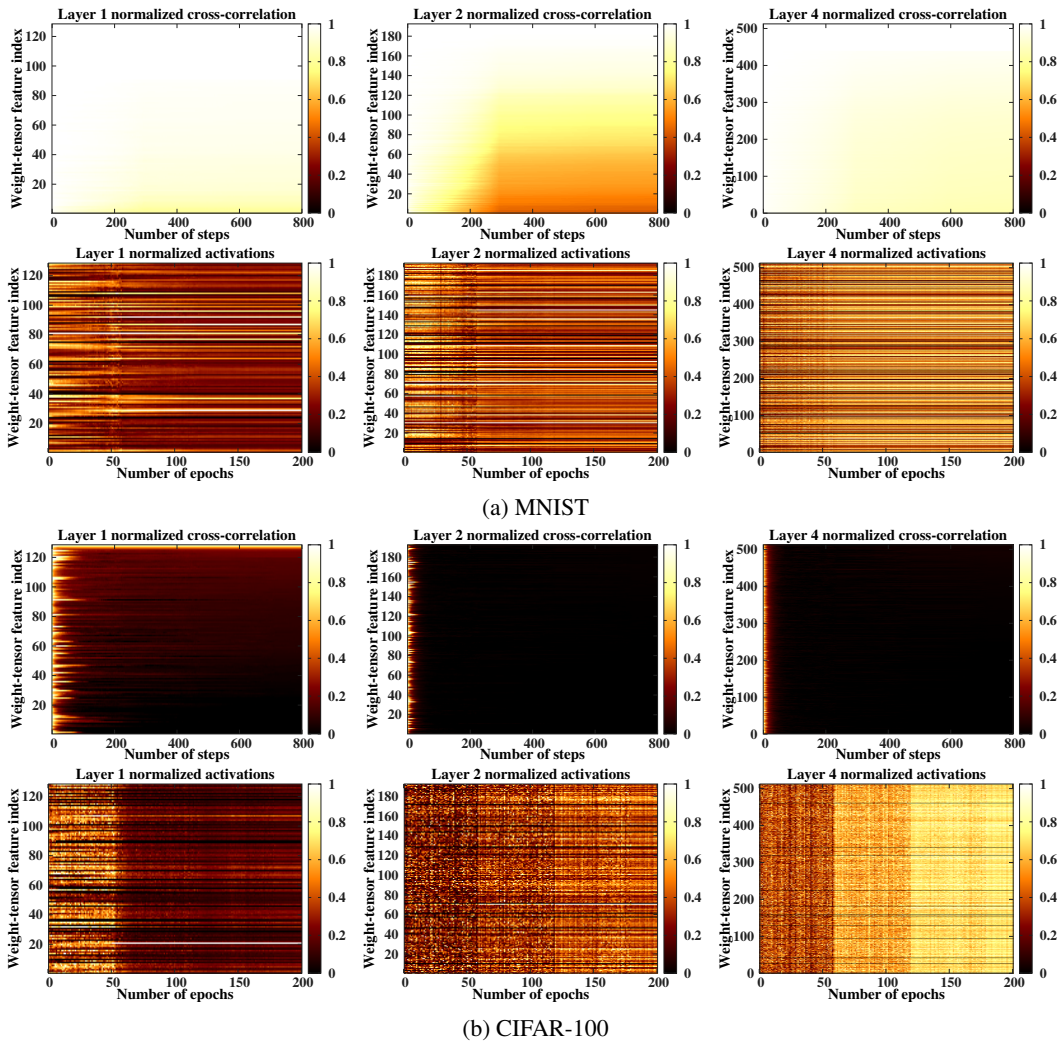


Figure 6: Time evolution of weight-tensor normalized cross-correlation for the CNN-3C-2FC architecture trained on the MNIST and CIFAR-100 datasets together with corresponding time evolution of normalized summed feature map activations for each epoch.

Weight distribution: In similar fashion we present the distribution of the weights in figure 7, featuring three distinct points of the pruning process depicted in figure 2. Specifically, we pick the original state containing all features, a state where all features were removed in one-shot corresponding to features that have not changed over time and the remaining features if layers were to be pruned to their maximum using individual thresholds. We observe that in all layers the shape of the distribution does not change when removing any feature and distributions do not become bimodal as would be the case if only low weight values were removed. Intuitively this is coherent with the definition of our metric, as we remove complete features that have not changed from their initial state and thus still follow the distribution applied in the initialization step of the network.

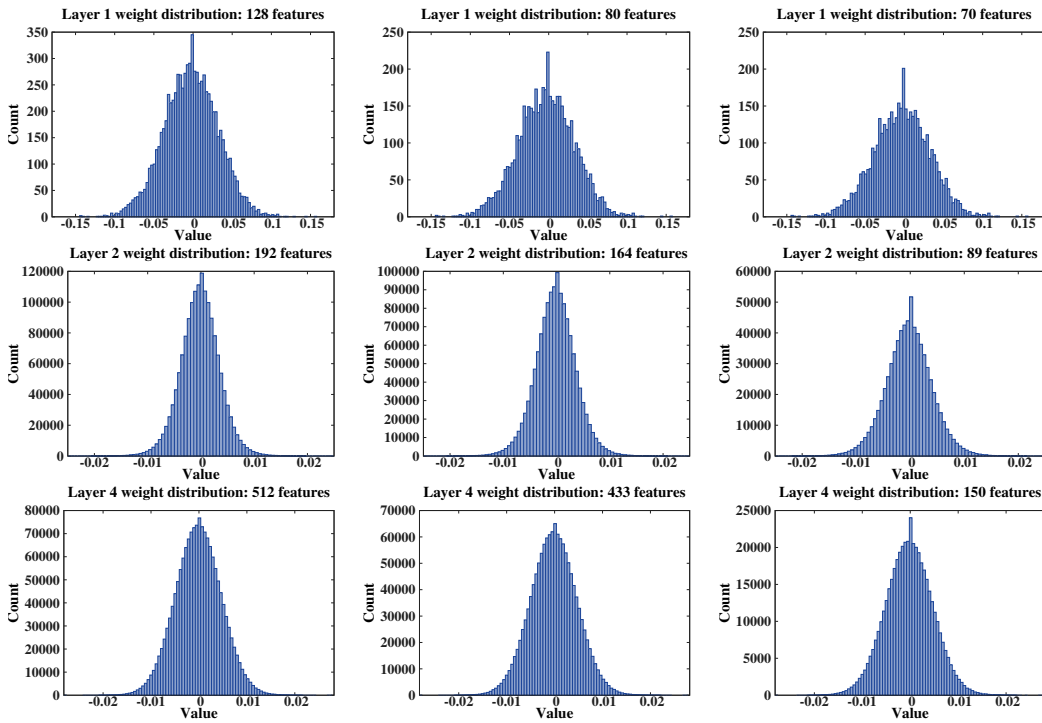
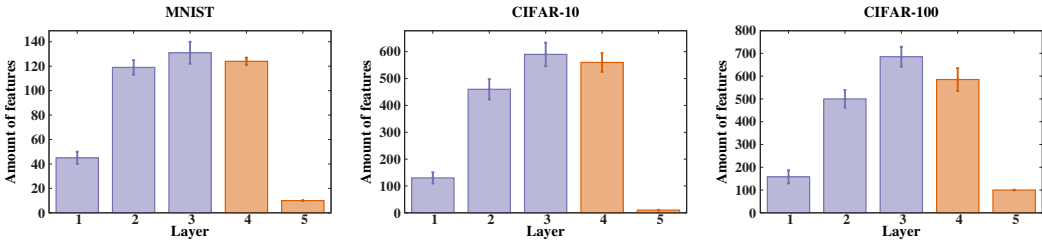


Figure 7: Weight distributions for the CNN-3C-2FC architecture trained on MNIST with initialization proposed by [13] at the different stages of pruning as shown in figure 2 . Note that we have rescaled the y-axis to emphasize that the shape of the distributions does not alter much.

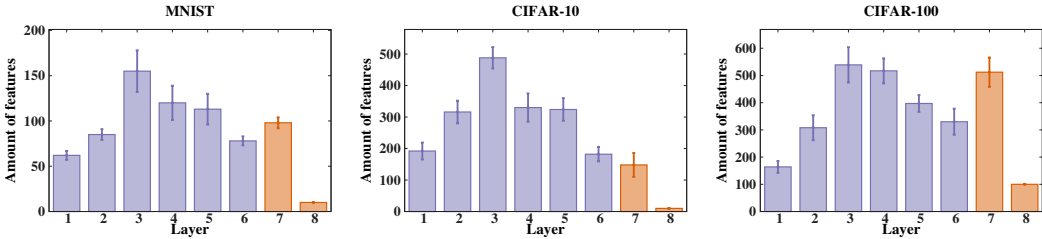
A.4 Automatically expanded architecture topologies

In addition to figure 4 we show mean evolved topologies including standard deviation for all architectures and datasets reported in table 1. In figure 8 and 9 all shallow and VGG architectures and their respective all-convolutional variants are shown. Figure 10 shows the evolved wide residual network architectures where blocks of layers are coupled due to the identity mappings. Wherever present, fully-connected layers are depicted in orange color.

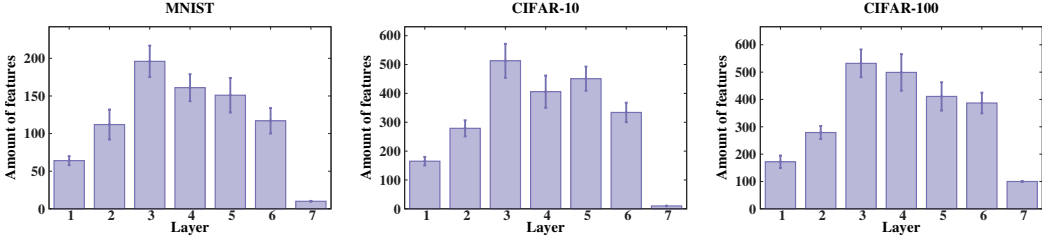
As already explained in the section on neural network topology formation we see that all evolved architectures feature topologies with maximum dimensionality in intermediate layers instead of in the highest layers of the architecture as usually present in conventional CNN design. For architectures where pooling has been replaced with larger stride convolutions we also observe that dimensionality of layers with sub-sampling changes independently of the prior and following convolutional layers suggesting that highly-complex pooling operations are learned. This an extension to the proposed all-convolutional variant of [17], where introduced additional convolutional layers were constrained to match the dimensionality of the previously present pooling operations.



(a) CNN-3C-2FC architecture

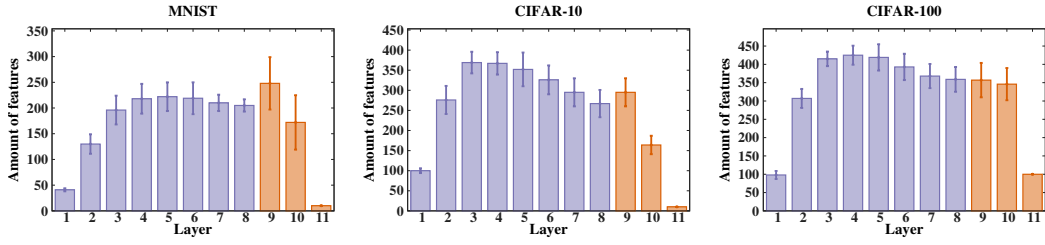


(b) all convolutional CNN-3C-2FC architecture with three additional larger stride convolutions replacing max-pooling operations

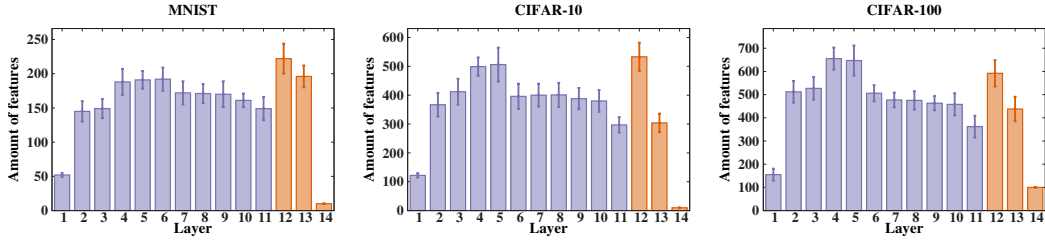


(c) all convolutional CNN-3C-2FC architecture with three additional larger stride convolutions replacing max-pooling operations without fully-connected layers and direct affine transformation to the class space from the last convolutional layer

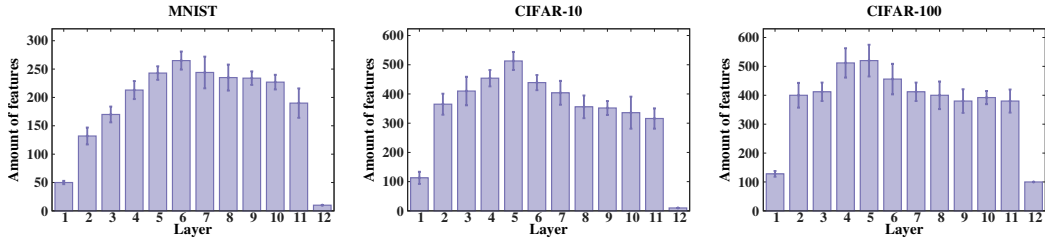
Figure 8: Mean and standard deviation of topologies as evolved from the expansion algorithm for the shallow networks run five times on MNIST, CIFAR-10 and CIFAR-100 datasets respectively.



(a) VGG-A architecture



(b) all convolutional VGG-A architecture with three additional larger stride convolutions replacing max-pooling operations



(c) all convolutional VGG-A architecture with three additional larger stride convolutions replacing max-pooling operations without fully-connected layers and direct affine transformation to the class space from the last convolutional layer

Figure 9: Mean and standard deviation of topologies as evolved from the expansion algorithm for the VGG-A style networks run five times on MNIST, CIFAR-10 and CIFAR-100 datasets respectively.

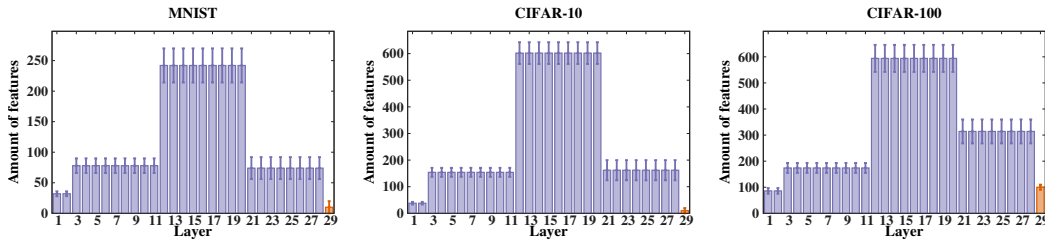


Figure 10: Mean and standard deviation of topologies as evolved from the expansion algorithm for the WRN-28 networks run five times on MNIST, CIFAR-10 and CIFAR-100 datasets respectively.